

***L1₀* ordering and microstructure of FePt thin films with Cu, Ag, and Au additive**

C. L. Platt,^{a)} K. W. Wierman, E. B. Svedberg, R. van de Veerdonk, and J. K. Howard
Seagate Research, 1251 Waterfront Place, Pittsburgh, Pennsylvania 15222-4215

A. G. Roy and D. E. Laughlin
Data Storage Systems Center, Carnegie Mellon University, Pittsburgh, Pennsylvania 15213-3890

(Received 10 July 2002; accepted 29 August 2002)

The influence of Cu, Ag, and Au additives on the *L1₀* ordering, texture, and grain size of FePt thin films has been examined. Lattice parameter data indicated that Au and Ag additives tended to segregate from FePt, but Cu alloyed with FePt. FePt films with Au or Ag additive showed 1–2 kOe higher coercivity values compared to a pure FePt film after annealing at 450 °C and above for 10 min. The addition of at least 20 vol. % Cu to FePt boosted average coercivity values and increased (001)/(002) x-ray peak intensity ratios, suggesting an accelerated *L1₀* ordering process for annealing temperatures exceeding 350 °C. Decreasing the film thickness promoted (001) film texture in FePt+20% Cu films, but higher annealing temperatures were required to achieve large coercivity. Au and Ag limited the average grain size compared to a pure FePt film. Cu additive increased the average grain size and film roughness. © 2002 American Institute of Physics.

[DOI: 10.1063/1.1516870]

I. INTRODUCTION

Areal recording densities in magnetic disk drives continue to advance at a rapid rate. Eventually, the physical limits of current media materials will be reached as average grain sizes are reduced to 5 nm and below to support large bit densities. The magnetocrystalline anisotropy of these materials must be high enough to prevent thermal decay of written information on magnetic recording media. FePt has generated much interest due to the high magnetocrystalline anisotropy ($K_u \approx 7 \times 10^7$ erg/cc) of its ordered tetragonal *L1₀* phase that develops at elevated temperatures (>550 °C).¹ By itself, FePt is not a viable media material because the requisite processing temperatures result in large grains (40–60 nm) that are highly exchange coupled. Additional agents are needed to tailor the thin-film microstructural and magnetic properties. Elements such as Cu (Ref. 2) and Zr (Ref. 3) have been added to FePt thin films to accelerate the *L1₀* ordering process such that useful magnetic properties can be achieved under less severe temperature and/or time requirements. Materials such as AlO_x,⁴ MgO,⁵ AlN,⁶ TaN,⁷ Ag,^{4,8} W,⁹ and Ti (Ref. 9) have shown promise in controlling FePt grain size in composite films. Other studies have shown that using Ni,¹⁰ B,¹⁰ BN,¹¹ or C (Ref. 11) additives can reduce the magnetic coupling in FePt.

Understanding the mechanism(s) by which these additives influence the *L1₀* ordering process would assist in the development of FePt media. Kitakami *et al.* reported that doping with Sn, Pb, Sb, or Bi reduced the *L1₀* ordering temperature of CoPt thin films, but Ag additive did not produce such an effect.¹² These additives were chosen because of their insolubility with Co and their low surface free en-

ergy; however, they do form stable alloys with Pt (except Ag) at or below the temperature of the bulk *L1₀* CoPt ordering temperature. Ostensibly, the ordering process in CoPt was aided by defects left in the film after the additive material diffused to the surface.

This study details the influence of highly diffusive Cu,² Ag,^{6,7,13} and Au additives on the microstructural and magnetic properties of FePt thin films. Cu has limited solubility in Fe, but it forms stable alloys with Pt at temperatures around 300 °C in the bulk. Both Ag and Au have low solubility with both Fe and Pt. Structural data indicated that the Cu additive alloyed with the FePt, but the Ag and the Au tended to diffuse out of the FePt lattice after annealing at progressively higher temperatures. Based on both structural and magnetic data, FePt films with Cu additive showed a greater degree of *L1₀* ordering than did pure FePt or FePt doped with Ag or Au for equivalent annealing conditions. The most remarkable differences were for films annealed at 350 °C. The diffusion/defect mechanism of the additive material does not fully account for the experimental observations. Therefore, it is proposed that the alloying of FePt and Cu is the mechanism responsible for accelerating the *L1₀* ordering process.

II. EXPERIMENTAL DETAILS

All thin films in this study were sputtered onto thermally oxidized Si(100) wafers at nominal room temperature. The sputter gas pressure was 3 mT for all layers in the film structure. A 5 nm MgO buffer layer rf sputtered at 200 W was used for all FePt films. Each additive was studied using a series of FePt+*x* vol. % {*x*=10, 20, 30, 40} metal composite films (20 nm) that were dc sputtered from an Fe₅₀Pt₅₀ alloy target and a separate Cu, Ag, or Au target. A reference FePt film (20 nm) was deposited without any additions.

^{a)}Electronic mail: christopher.l.platt@seagate.com

Postdeposition annealing was performed in flowing Ar in a rapid thermal processor at 350, 450, 550, and 650 °C for 10 min. Structural properties were measured using standard θ - 2θ x-ray diffraction (XRD) with a Cu source ($\lambda=1.54$ Å) and x-ray mirror optics. XRD peak intensities and peak positions were determined by fitting to a pseudo-Lorentzian profile. In the case of peak doublets, a double Lorentzian profile was used. Hysteresis loops up to 1.8 T were measured with a polar magneto-optical Kerr effect magnetometer. Images of the surface topology were obtained with a Digital Instruments atomic force microscope (AFM) operating in tapping mode. Images were taken with a frequency of 1 Hz and a resolution of 512×512 pixels over $2\times 2 \mu\text{m}$ with a standard Si tip. Selected samples were prepared for plan-view or cross-section transmission electron microscopy (TEM) by polishing and ion milling.

III. RESULTS AND DISCUSSION

High-angle XRD was used to correlate changes in fiber texture with both the volume fraction and type of additive. Figure 1 compares XRD data for the MgO (5 nm)/FePt+ x vol. % $\{x=10,20,30,40\}$ (20 nm) additive samples annealed for 10 min at 650 °C. The expected positions of the ordered FePt peaks and any peaks from the additive materials are labeled. Evidence of $L1_0$ ordering was signified by the appearance of the (001) chemically ordered FePt peak and the tetragonal (200) and (002) peaks. The position of the ordered tetragonal (111) peak is only slightly shifted from the position of the cubic (111) peak upon ordering. Therefore, it is more difficult to monitor the $L1_0$ transformation process from the (111) peak position. The reference film (not shown) showed a preferred (111) orientation in both as-deposited and annealed states. The Cu additive [Fig. 1(a)] enhanced the (001) texture in the FePt, although a distinct (200) tetragonal peak also was evident. Trends in peak intensities with varying composition reflected changes in either texture or grain size. The FePt(002) peak shifted closer to the expected position of the Cu(200) peak ($2\theta=50.5$ °) with increasing volume fraction of Cu. The FePt films with Ag additive [Fig. 1(b)] showed a stronger (200) component to the texture and less splitting between the (200) and (002) peaks than the Cu-doped films. The Au intensified the FePt(111) texture as evidenced by the diminished (001) and (200)/(002) reflections [Fig. 1(c)]. Note that elemental Ag and Au peaks were present in the XRD scans for the films with large fractions of additive. These elemental peaks were not observed in the as-deposited films. Rather, the (111) Ag and (111) Au peaks grew in intensity as a function of increasing anneal temperature, suggesting an increasing accumulation of the elemental phases of the additive material with annealing. No elemental Cu peaks were detected for concentrations up to 40 vol. % [Fig. 1(a)]. This observation, coupled with the noted shift of the FePt(002) peak, provide evidence of FePt–Cu alloying.

Changes in the FePt cell dimensions were also seen as a result of the different diffusion and alloying mechanisms of the various additives. An average d spacing was calculated from the position of the FePt(200) peak for films with the various additives after annealing at different temperatures for

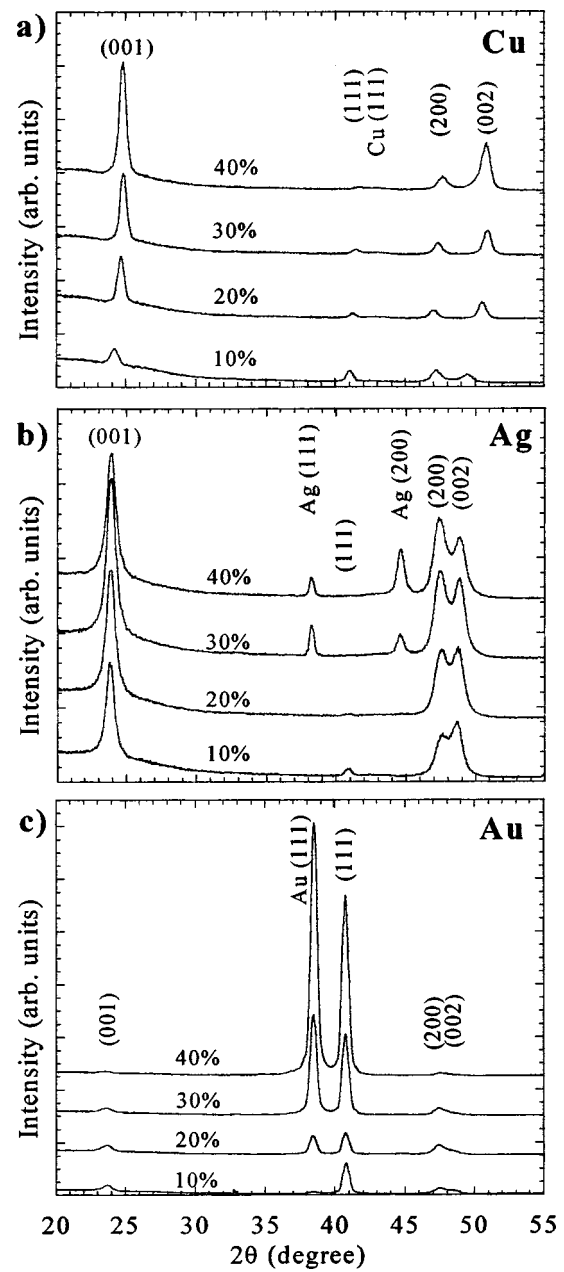


FIG. 1. XRD scans of (a) MgO (5 nm)/FePt+ x % Cu, (b) MgO (5 nm)/FePt+ x % Ag, (c) MgO (5 nm)/FePt+ x % Au additive (20 nm) $\{x=10, 20, 30, 40\}$ annealed 650 °C/10 min.

10 min (Fig. 2). The y -axis scaling in Fig. 2 is identical so that the magnitude of the changes in d spacing can be compared. The (200) peak was chosen because that peak was observable for all of the films in the study. The data for the reference sample are plotted in each panel for comparison. The (200) d spacing for the reference sample decreased by about 1%, comparing the 350 and 650 °C data, owing to the slight tetragonal distortion of the $L1_0$ phase. The (200) d spacing was smaller for the FePt films with Cu additive after the 350 °C anneal [Fig. 2(a)]. An approximate 1% increase in the d spacing was observed for the Cu-doped films with increasing anneal temperature. There was a large difference between the data for the 30 and 40 vol. % Cu films, which may have resulted from a change in the details of the

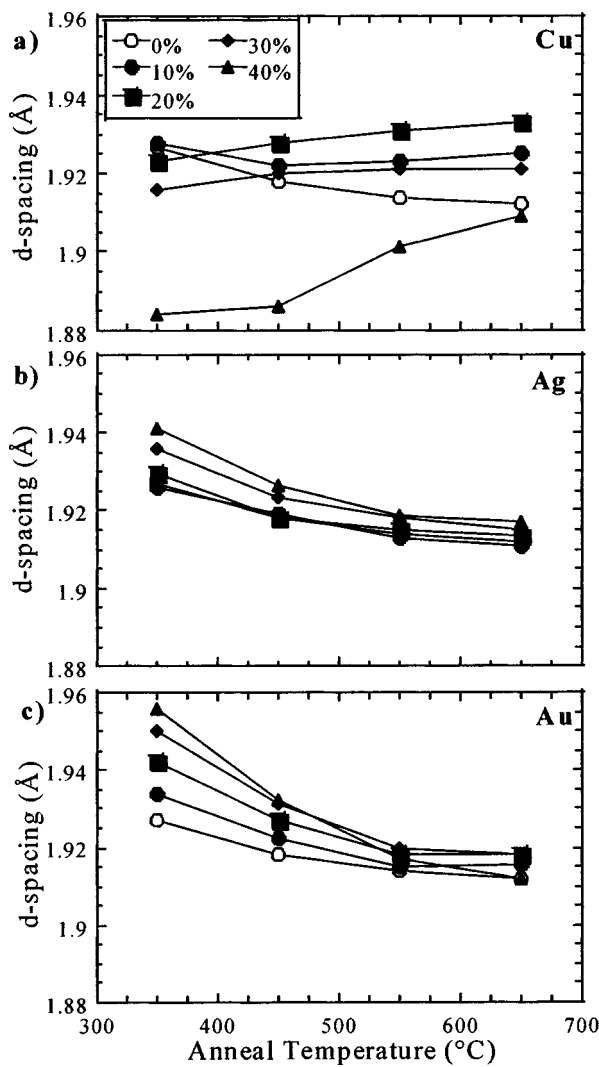


FIG. 2. d spacing calculated from (200) peak position vs annealing temperature for MgO (5 nm)/ $\text{FePt}+x\%$ additive (20 nm) film series with (a) Cu, (b) Ag, and (c) Au. Annealing time was 10 min.

FePt–Cu alloying, i.e., the composition and volume fraction of particular alloys that were forming.

The more Ag or Au added to the FePt, the larger the (200) d spacing increased above the reference level [Figs. 2(b) and 2(c)]. This was due to the initial expansion of the lattice by the larger Ag or Au atoms. Note that Au expanded the lattice more than Ag. After annealing at higher temperatures, the d -spacing data of the Ag or Au-doped films converged to a value closer to the reference. These results are consistent with the idea that the Ag and Au additives were diffusing out of the FePt lattice either to the film surface or into the grain boundaries.

As mentioned previously, the $L1_0$ ordering process results in a tetragonal distortion of the FePt unit cell, resulting in a c/a ratio that is less than 1. From the positions of the (200) and (002) XRD peaks, average values for the a - and c -lattice parameters, respectively, were calculated for the films with Cu and Ag additives [the (002) peak was not observable in the films with Au due to the strong (111) texture]. A c/a ratio was determined, although the value is only reflective of average values of c - and a -lattice parameters

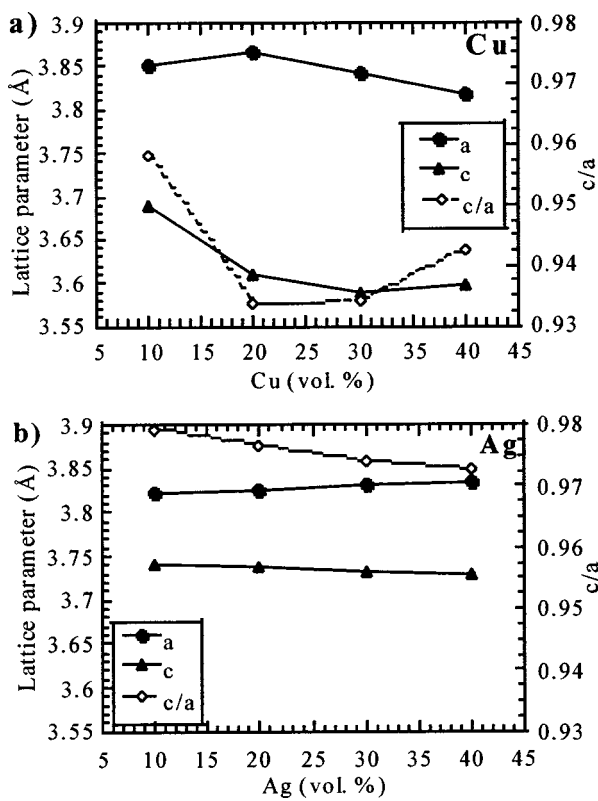


FIG. 3. a - and c -lattice parameters and c/a ratios for (a) MgO (5 nm)/ $\text{FePt}+x\%$ Cu (20 nm) films and (b) MgO (5 nm)/ $\text{FePt}+x\%$ Ag (20 nm) films ($x=10, 20, 30, 40$) annealed at $650^\circ\text{C}/10$ min.

from different grains. Figures 3(a) and 3(b) plot lattice parameter data and c/a ratio versus additive volume fraction for FePt films with Cu and Ag additive annealed at 650°C for 10 min (note: equivalent scaling in plots). Bulk $L1_0$ FePt values for a - and c -lattice parameters are given as 3.852 and 3.713 Å, respectively.¹³ The bulk c/a ratio is 0.964. The FePt+Ag samples showed comparable values to the published bulk numbers; however, the FePt+Cu samples showed a decreasing c -lattice parameter with increasing Cu concentration up to 30 vol. %. This reduced the c/a ratio to approximately 0.935. The results for the 40 vol. % Cu film were, again, slightly anomalous.

Figure 4 takes a different look at the texture development and $L1_0$ ordering of the FePt+Cu films by examining the trends in the (a) (002)/(200) and (b) (001)/(002) XRD peak intensity ratios as a function of annealing temperature. Fitted peak intensities were used rather than peak areas to simplify the calculation, since overall peak shapes were similar and only slight variations in the data would result from integrating the peaks. Figure 4(a) shows that as the concentration of Cu in the film increased, the gradient of the (002)/(200) peak intensity ratio with annealing temperature also increased. Thus, increasing the amount of Cu improved the perpendicular orientation of the $L1_0$ -ordered FePt. The ratio of the (001) superlattice peak to the (002) fundamental peak is an indication of the degree of chemical ordering in FePt, i.e., the periodic layer-by-layer arrangement of Fe and Pt atoms. The (001)/(002) peak intensity ratio data in Fig. 4(b) show that increasing the volume fraction of Cu improved the

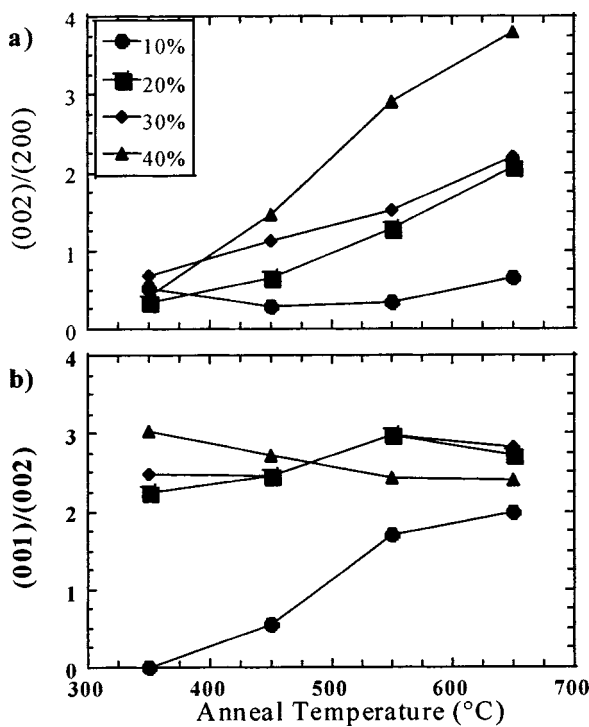


FIG. 4. (a) (002/200) and (b) (001/002) peak intensity ratios vs annealing temperature for MgO (5 nm)/FePt+ $x\%$ Cu (20 nm) films.

chemical ordering the FePt, especially at the lower end of the range of annealing temperatures. Adding too much Cu (40%) resulted in a slight degradation of chemical ordering with increasing anneal temperature.

The trends revealed in the XRD data were supported by magnetic measurements. It has been demonstrated that film coercivity (H_c) increases with the volume fraction of $L1_0$ -ordered grains relative to disordered grains.¹⁴ The influence of grain growth on H_c must also be considered since the $L1_0$ transformation requires high-temperature treatments.¹⁵ Figure 5 shows the variation of perpendicular H_c with annealing temperature for the different series of FePt+additive films. The data for the reference sample are also plotted within each panel for comparison. The addition of Cu, Ag, or Au increased the H_c of FePt above the reference values for equivalent annealing conditions. Clearly, the relative influence of the Cu additive on the FePt H_c was much more significant than the Ag or Au additives at the low end of the range of annealing temperatures. The small increase in H_c for the FePt with Ag or Au additive was possibly the result of reduced magnetic coupling.⁴ The substantial increase in perpendicular H_c for FePt+Cu is consistent with the decreased c/a ratio [Fig. 3(a)], better perpendicular orientation [Fig. 4(a)], and more complete $L1_0$ chemical ordering [Fig. 4(b)].

The structural and magnetic data discussed thus far were for 20 nm films. Actual magnetic recording media would likely be much thinner. It was discovered that the texture and H_c of the FePt+Cu films varied with total film thickness. Therefore, the relationship between FePt+Cu film thickness and the $L1_0$ ordering process was also investigated. The FePt+20% Cu composition was chosen for this part of the study since it represented the minimum amount of Cu needed to

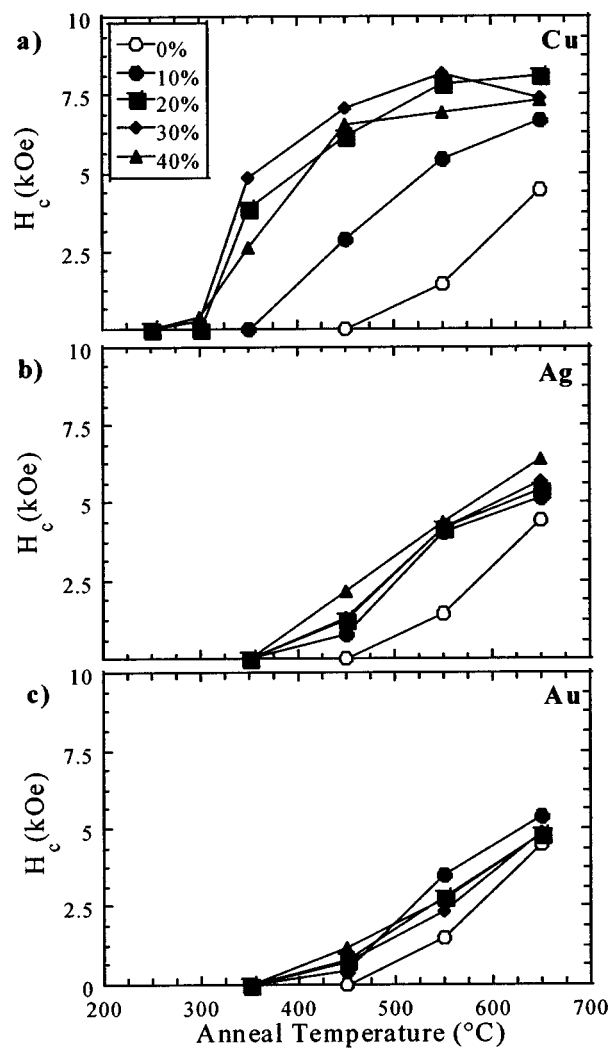


FIG. 5. H_c vs annealing temperature for MgO (5 nm)/FePt+additive (20 nm) film series with (a) Cu, (b) Ag, and (c) Au.

significantly accelerate the ordering process. Figure 6 shows the high-angle XRD scans for films of FePt+20% Cu with different thicknesses that were annealed at 650 °C for 10 min. Differences in film stress associated with the change in thickness likely affected the development of texture upon

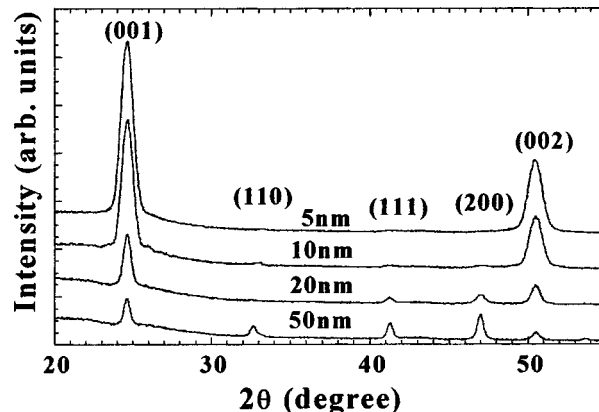


FIG. 6. XRD scans of MgO (5 nm)/FePt+20% Cu films with varying total thicknesses annealed 650 °C/10 min.

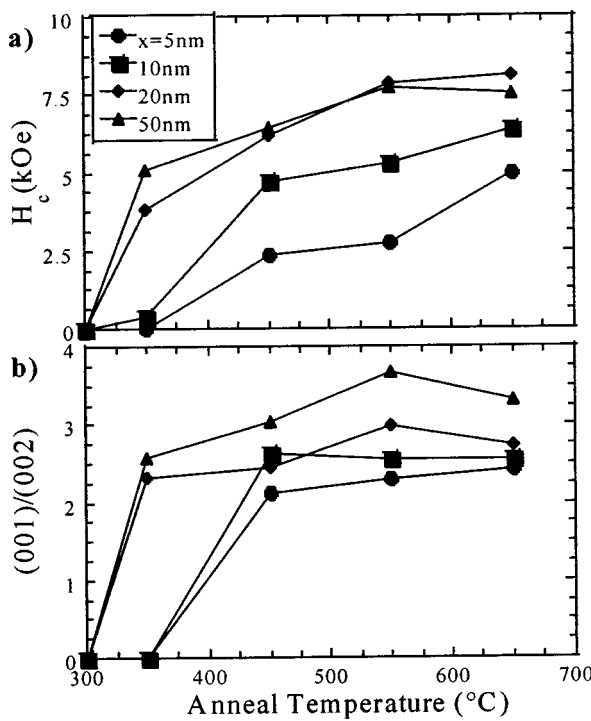


FIG. 7. (a) H_c vs annealing temperature and (b) (001/002) peak intensity ratios vs annealing temperature for MgO (5 nm)/FePt+20% Cu (x) films with varying total thicknesses.

annealing.¹⁶ Clearly, the (001) texture was improved for decreasing film thickness. The thicker films developed a more random texture. The (a) perpendicular H_c and (b) (001)/(002) XRD peak intensity ratio data are plotted versus annealing temperature in Fig. 7 for the FePt+20% Cu thickness series. Both Figs. 7(a) and 7(b) indicate that the 5 nm film did not transform to the degree of the thicker films under equal annealing conditions. One possible explanation for this is that film thickness is limiting the grain size, which may be inhibiting the $L1_0$ ordering.⁴

An initial survey of film microstructure of the various annealed films was performed with an atomic force microscope. This technique is faster and less involved than TEM and shows trends in grain size and film roughness. The 20 vol. % additive samples were examined after various annealing treatments and compared with the reference sample annealed under the same conditions. Figure 8 shows $1 \times 2 \mu\text{m}$ images of the surface morphology for the different films after the $650^\circ\text{C}/10\text{ min}$ anneal. The annealed FePt+Cu film [Fig. 8(a)] was significantly rougher than the other films. The rms surface roughness was derived from the complete set of images, including the lower annealing temperatures. Figure 9 shows the dependence of rms roughness on the annealing temperature. The general trend of increasing roughness with annealing temperature was expected based on grain growth. The films with Ag and Au additive were slightly rougher than the reference after the lower temperature anneals, but they were smoother than the reference after the $650^\circ\text{C}/10\text{ min}$ anneal.

The XRD and AFM data indicated that the different additives had distinct effects on the microstructure. TEM was used to compare the trends in the AFM data with average

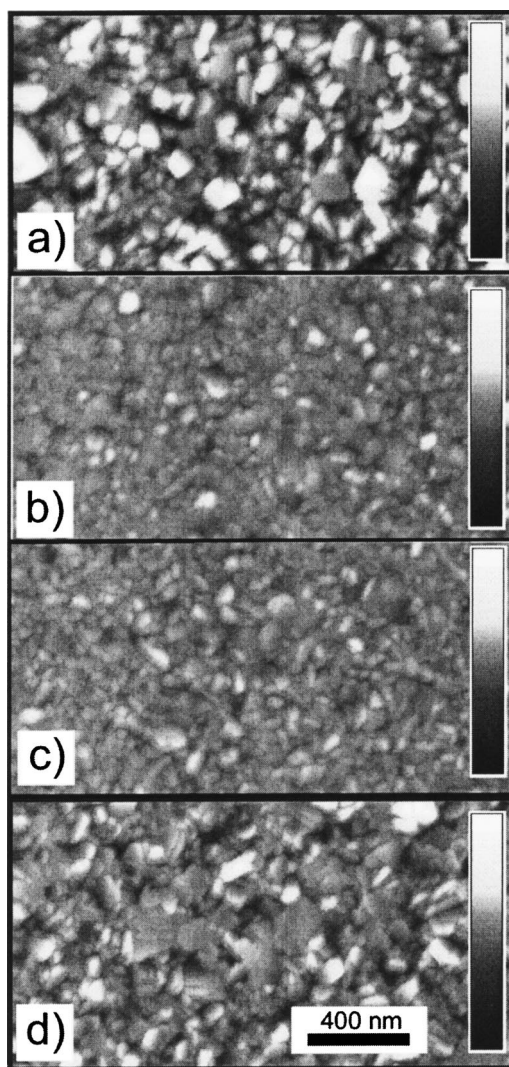


FIG. 8. AFM images of $650^\circ\text{C}/10\text{ min}$ annealed MgO (5 nm)/FePt+20% additive (20 nm) films with (a) Cu, (b) Ag, (c) Au, and (d) reference.

grain size. Also, based on conclusions made from the XRD data that Cu was alloying and Ag and Au were diffusing out of the FePt lattice, it was desired to determine whether the additive materials were traveling to grain boundaries or to the surfaces of the films upon annealing. Figure 10 shows

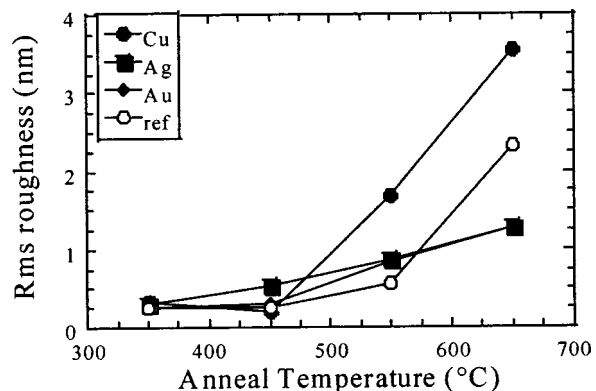


FIG. 9. Rms roughness vs annealing temperature for MgO (5 nm)/FePt+20% additive (20 nm) film series.

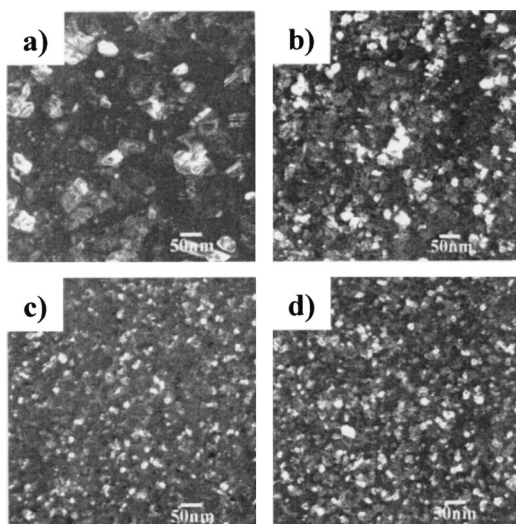


FIG. 10. Plan-view dark-field TEM images of 450 °C/10 min annealed MgO (5 nm)/FePt+20% additive (20 nm) films with (a) Cu, (b) Ag, (c) Au, and (d) reference.

dark-field TEM micrographs of the MgO(5 nm)/FePt+20% additive (20 nm) films in comparison with the reference film. All samples were annealed at 450 °C for 10 min. Each image was obtained by selected aperture over the (200) diffraction ring. The 450 °C anneal was chosen as a stage of interest since many of the magnetic and structural parameters of the FePt+20% Cu sample were significantly developing by this point, albeit the samples with the other additives indicated only limited $L1_0$ ordering. The average grain size for the FePt+20% Cu sample [Fig. 10(a)] was 50 nm, compared to 24 nm for the FePt+Ag, 14 nm for the FePt+Au, and 20 nm for the reference. These data do not correlate well with the AFM data for these annealing conditions, but they are closer in comparison with the AFM data at 550 °C or above. Clearly, the larger grain size of the FePt+Cu films resulted in noticeable increases in film roughness. Rather, the grain size data compares better with the H_c data of Fig. 5, suggesting a correlation between $L1_0$ transformation, grain growth, and H_c .

Chemical analysis was performed on the TEM samples (plan view and/or cross section) of the annealed films using either energy dispersive x rays (EDX) or electron energy loss spectroscopy. Film composition data were not extracted from the EDX scans. Rather, location of the additive species was the primary focus of the measurements. The EDX data on the cross-sectioned FePt+Au film indicated that Au had migrated toward the surface of the film or to the interface with the MgO buffer. In the FePt+Cu samples, no evidence was found for accumulation of Cu at grain boundaries or at the

film surface. This is consistent with the conclusion that Cu was alloying with FePt. So far, no decisive conclusion has been made about the behavior of the Ag additive based on the chemical analysis. Ag appeared to be evenly dispersed, but the relative signal intensity was weak compared to samples with the other additives.

IV. CONCLUSIONS

The effects of Cu, Ag, or Au additions on the $L1_0$ ordering and grain growth of thin FePt films have been studied. The Ag and the Au additives affected the structural and magnetic properties of FePt in a similar manner. The XRD data suggest that both Ag and Au tended to chemically segregate from FePt. This likely explains the smaller average grain size of the annealed FePt+Ag and FePt+Au films compared to FePt+Cu. The most significant improvement on the $L1_0$ ordering process was observed in films with Cu additions above 20 vol. %. The XRD data suggest that Cu alloys with FePt. The formation of FePt–Cu alloy(s) may be a driving force behind the accelerated $L1_0$ kinetics in these films. The FePt+Cu films showed a tendency to develop a (001) texture that improved with decreasing film thickness. Decreasing film thickness, however, reduced the rate of the $L1_0$ ordering process. Further understanding of the interdependence of $L1_0$ ordering, stoichiometry, texture development, and grain growth in thin films is needed.

- ¹K. Coffey, M. A. Parker, and J. K. Howard, IEEE Trans. Magn. **31**, 2737 (1995).
- ²T. Maeda, T. Kai, A. Kikitsu, T. Nagase, and J. Akiyama, Appl. Phys. Lett. **80**, 2147 (2002).
- ³S.-R. Lee, S. Yang, Y. K. Kim, and J. G. Na, Appl. Phys. Lett. **78**, 4001 (2001).
- ⁴D. H. Ping, M. Ohnuma, K. Hono, M. Watanabe, T. Iwasa, and T. Masumoto, J. Appl. Phys. **90**, 4708 (2001).
- ⁵T. Suzuki and K. Ouchi, IEEE Trans. Magn. **37**, 1283 (2001).
- ⁶S. C. Chen, P. C. Kuo, C. T. Lie, and J. T. Hua, J. Magn. Magn. Mater. **236**, 151 (2001).
- ⁷T. Shimatsu, J. C. Lodder, Y. Sugita, and Y. Nakamura, IEEE Trans. Magn. **35**, 2697 (1999).
- ⁸S.-C. Chen, P. C. Kuo, A. C. Sun, C. T. Lie, and W. C. Hsu, Mater. Sci. Eng., B **88**, 91 (2002).
- ⁹C.-M. Kuo, P. C. Kuo, W.-C. Hsu, C.-T. Li, and A.-C. Sun, J. Magn. Magn. Mater. **209**, 100 (2000).
- ¹⁰N. Li, B. M. Lairson, and O.-H. Kwon, J. Magn. Magn. Mater. **205**, 1 (1999).
- ¹¹J. A. Christodoulides, P. Faber, M. Daniil, H. Okumura, G. C. Hadjipanayis, V. Skumryev, A. Simopoulos, and D. Weller, IEEE Trans. Magn. **37**, 1292 (2001).
- ¹²O. Kitakami, Y. Shimada, K. Oikawa, H. Daimon, and K. Fukamichi, Appl. Phys. Lett. **78**, 1104 (2001).
- ¹³JCPDS-International Centre of Diffraction Data (1999).
- ¹⁴R. A. Ristau, K. Barmak, L. H. Lewis, K. R. Coffey, and J. K. Howard, J. Appl. Phys. **86**, 4527 (1999).
- ¹⁵E. F. Kneller and F. E. Luborsky, J. Appl. Phys. **34**, 656 (1963).
- ¹⁶V. Karanasos, I. Panagiotopoulos, D. Niarchos, H. Okumura, and G. C. Hadjipanayis, Appl. Phys. Lett. **79**, 1255 (2001).